

See discussions, stats, and author profiles for this publication at: <https://www.researchgate.net/publication/257347307>

# Flow, packing and compaction properties of novel coprocessed multifunctional directly compressible excipients prepared from tapioca starch and mannitol

Article in *Pharmaceutical Development and Technology* · October 2013

DOI: 10.3109/10837450.2013.840843 · Source: PubMed

CITATIONS

29

READS

1,231

2 authors:



Oluwatomide Adeoye

University of Lisbon

16 PUBLICATIONS 414 CITATIONS

SEE PROFILE



Gbenga Alebiowu

Obafemi Awolowo University

38 PUBLICATIONS 449 CITATIONS

SEE PROFILE

Some of the authors of this publication are also working on these related projects:



A Study of Co-processed Binders as Excipients in a Paracetamol Tablet Formulation [View project](#)



Encapsulation of Probiotic Based Nutraceuticals from Bambara Groundnut [View project](#)

RESEARCH ARTICLE

# Flow, packing and compaction properties of novel coprocessed multifunctional directly compressible excipients prepared from tapioca starch and mannitol

Oluwatomide Adeoye and Gbenga Alebiowu

*Department of Pharmaceutics, Faculty of Pharmacy, Obafemi Awolowo University, Ile-Ife, Nigeria*

## Abstract

Novel multifunctional excipients were prepared by coprocessing tapioca starch with mannitol using two methods viz; co-grinding and co-fusion. The flow, packing and compaction properties of the native and novel excipients were evaluated by using density, Hausner's ratio, angle of repose, the maximum volume reduction, consolidation index, the rate of consolidation, angle of internal friction, morphological properties, Heckel analysis, tensile strength and dilution potential as evaluation parameters. The study revealed that the method of coprocessing, particle size and particle shape influenced the properties of the resulting novel excipients. Co-grinding was less effective than co-fusion in the preparation of excipients with enhanced properties. The study concluded that coprocessing tapioca starch and mannitol will enhance the flow, packing and compaction properties of the novel excipient and that the co-fusion method of coprocessing would produce novel excipients with enhanced direct compression potential compared to the co-grinding method.

## Keywords

Angle of internal friction, compaction properties, consolidation index and rate of consolidation, direct compression, maximum volume reduction

## History

Received 12 February 2013

Revised 15 August 2013

Accepted 16 August 2013

Published online 3 October 2013

## Introduction

Tablets are the most common and preferred dosage form because of the ease of manufacturing, stability, dose uniformity and patient acceptability. The evolution of tablet manufacturing into a science is mainly a result of increased therapeutic demand for the dosage form and the consequent introduction of high speed tableting machines and direct compression. The simplicity and cost effectiveness of direct compression has made it the preferred method for the preparation of tablets, thus placing high functionality demands on the pre-compression blend for flowability and compressibility. Despite the paucity of directly compressible active pharmaceutical ingredients (APIs) and excipients, direct compression has continued to gain popularity and increased use in the pharmaceutical industry<sup>1–3</sup>.

Over the past two decades, increased research activities in the field of tablet excipient development and manufacturing have been directed towards the discovery and manufacture of highly functional (multifunctional) directly compressible excipients that will reduce the number of excipients and potential interaction between excipients in a formulation. One important method of manufacturing such an excipient is coprocessing; a science of particle engineering by which two or more excipients are combined into a single multifunctional excipient with superior intrinsic performance such as high compatibility, high intrinsic flow, good binding properties, improved lubricating efficiency and dilution potential<sup>2,4,5</sup>.

Powder fluidity (or flowability), which is one of the important requirements of a directly compressible excipient is a complex property and its multidimensional nature makes it difficult to be characterized holistically by a single method. Thus, a number of methods, each concentrating on a particular aspect or principle of powder flow, have been used to characterize flowability. These methods include the measurement of the powder flow through an orifice; angle of repose; packing and cohesive properties, angle of internal friction (AIF) of powders; bulk and tapped densities of powders; the energy to stir powder bed etc.<sup>6–8</sup>. The packing and cohesive properties of bulk powders are important characteristics that affect powder storage, powder flow, die filling during compression and bulk powder compaction<sup>9,10</sup>. Weight uniformity, tablet performance and process design can all be optimized with an adequate knowledge of powder packing behaviour<sup>11</sup>. Powder packing and powder flow, as physical properties of bulk powders are affected by fundamental properties such as particle shape and size<sup>12,13</sup>.

The aim of the present study was to coprocess tapioca starch (TPS; having binding, disintegrating and diluent properties)<sup>14,15</sup> with mannitol (MNT; having rapid dissolution, taste masking and diluent properties)<sup>2,16</sup> using two methods (co-fusion and co-grinding) and to evaluate the properties of the resulting products along with the native excipients. This study also proposed to determine whether a mixture of the product obtained from the two methods would yield a product with properties different from the starting products.

## Materials and methods

The materials used were MNT (BDH Chemicals Ltd., Poole, UK), acetone (Sigma–Aldrich Laborchemickalien GMBH, Seelze,

Address for correspondence: Gbenga Alebiowu, Department of Pharmaceutics, Faculty of Pharmacy, Obafemi Awolowo University, Ile-Ife 234036, Nigeria. E-mail: gbengaalaba@gmail.com

Germany) and TPS (prepared in our laboratory from tubers of *Mannihot utilisima* L.).

### Extraction of TPS

The TPS was extracted from the root tubers of cassava (*M. utilisima* L.) using established procedures<sup>17</sup>. The cassava tubers were peeled, washed and cut into small pieces which were soaked in distilled water for 48 h for softening. The softened tubers were milled to a pulp, and distilled water was added to dilute the slurry which was then sieved using a 100 µm mesh. The procedure was repeated three times until starch was fully extracted from the tubers as confirmed by negative iodine test on the remaining chaff. The extracted starch was dried at 50 °C in hot air oven (Gallenkamp, Model OV-335, Vindon Scientific Ltd, Oldham, UK) for 72 h. The dried mass was powdered in a laboratory mill (Christy and Norris Ltd, Chelmsford, UK) at a speed of 1200 rpm using a screen size of 250 µm. This was carried out at a room temperature of 28 °C and the product was stored in a screw-capped bottle until needed.

### Coprocessing by co-fusion

Equal amounts of dried MNT and TPS were fused together by dispersing the TPS in distilled water already heated to 50 °C. The dispersion was then stirred for 5 min at the same temperature to form a paste. The dry MNT powder was then added to the TPS paste and mixed together by stirring on a hot plate (40 °C) for 10 min. The resulting paste (fused MNT and TPS) was then dried at 50 °C in a hot air oven for 24 h before it was milled and sieved using a 250 µm sieve. The coprocessed product (FTM) was stored in a screw-capped bottle until needed.

### Coprocessing by co-grinding

An equal amount, each of dried MNT and TPS was used. The MNT and TPS were triturated together using a porcelain mortar and pestle for 10 min to ensure a uniform size reduction and mixing of the two powders<sup>18</sup>. The resulting product (GTM) was passed through a 250 µm sieve and stored in a screw-capped bottle until needed.

### Co-grinding of the co-fused and co-ground excipients

The coprocessed excipients, i.e. those obtained by co-fusion and co-grinding were further coprocessed by co-grinding together using porcelain mortar and pestle. Different ratios, i.e. 1:3, 1:1 and 3:1 of GTM and FTM excipients were used for this process to produce CFG 1, CFG 2 and CFG 3, respectively. The products were stored in screw-capped bottles until needed.

### Determination of particle shape and size

The particle size and shape of each excipient was determined by optical microscopy (LEICA DM 750 Research Microscope with an integrated icc50 camera, LEICA Microsystems GmbH, Wetzlar, Germany) on 500 particles randomly selected from the optical field. The photomicrographs taken (Figures 1–7) were analyzed using the Image-pro Premier software (MediaCybernetics, Bethesda, MD). The size and shape descriptors used in this study are defined below<sup>11,19</sup>;

$$\text{Equivalent circle diameter (ECD)} = 2\sqrt{\frac{A}{\pi}} \quad (1)$$

$$\text{Aspect ratio (AR)} = \frac{b}{l} \quad (2)$$

$$\text{Roundness (RD)} = \frac{4\pi A}{p^2} \quad (3)$$

$$\text{Irregularity (IR)} = \frac{p}{l} \quad (4)$$

$$\text{Elongation ratio (ER)} = \frac{l}{b} \quad (5)$$

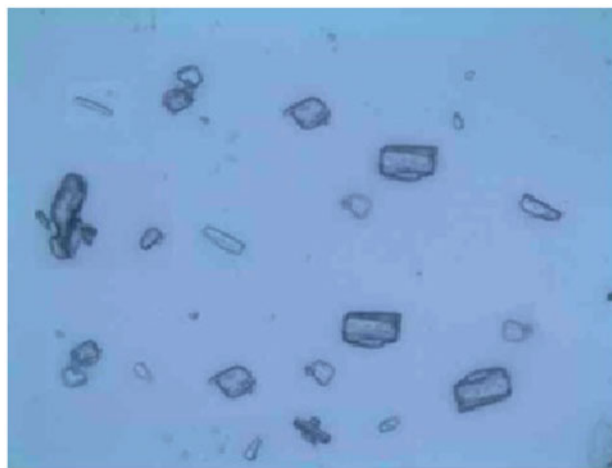


Figure 1. Photomicrograph of mannitol (MNT) powder (×400).

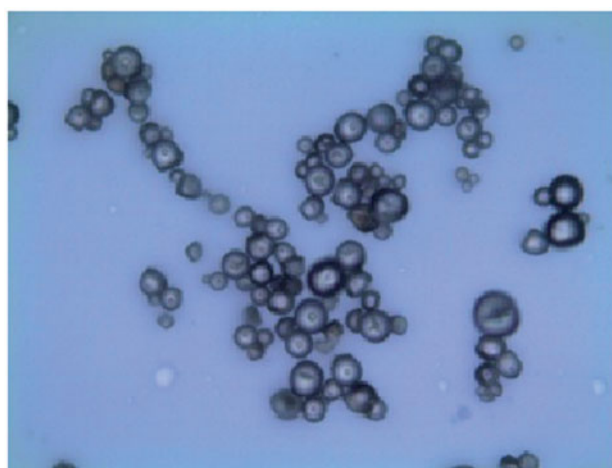


Figure 2. Photomicrograph of tapioca starch (TPS) powder (×400).

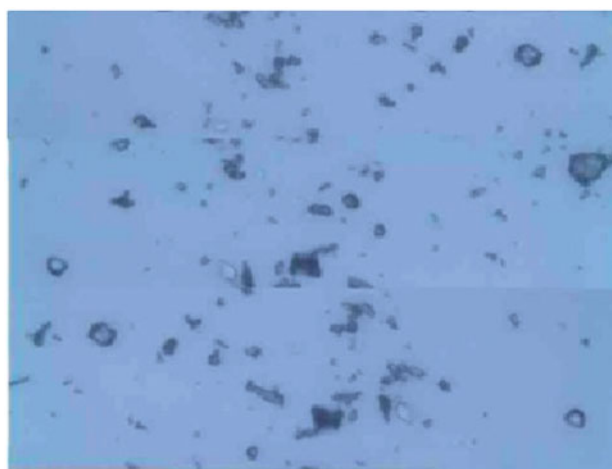


Figure 3. Photomicrograph of FTM powder (×400).

where

$b$  = minimum Feret diameter

$l$  = maximum Feret diameter

$A$  = projected area of the particle

$p$  = perimeter of the particle.

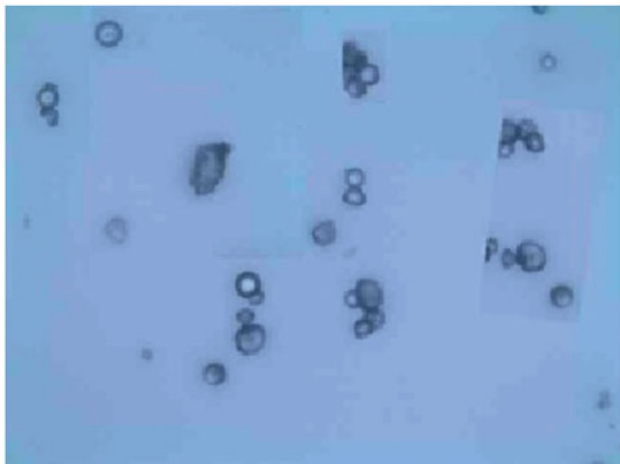


Figure 4. Photomicrograph of GTM powder ( $\times 400$ ).

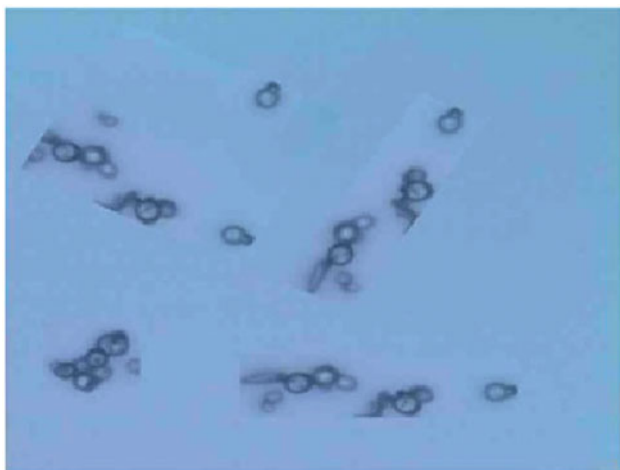


Figure 5. Photomicrograph of CFG 1 powder ( $\times 400$ ).

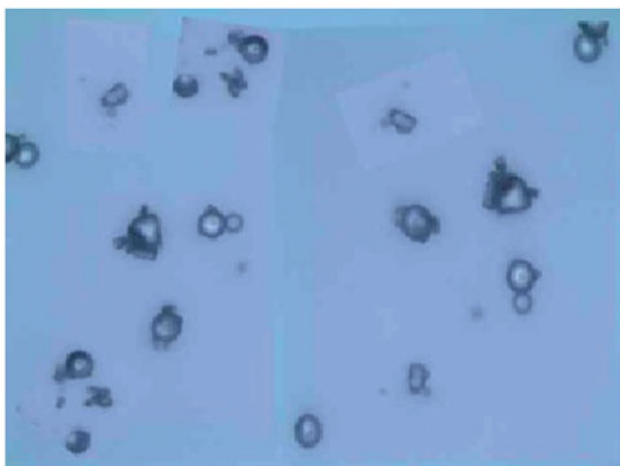


Figure 6. Photomicrograph of CFG 2 powder ( $\times 400$ ).

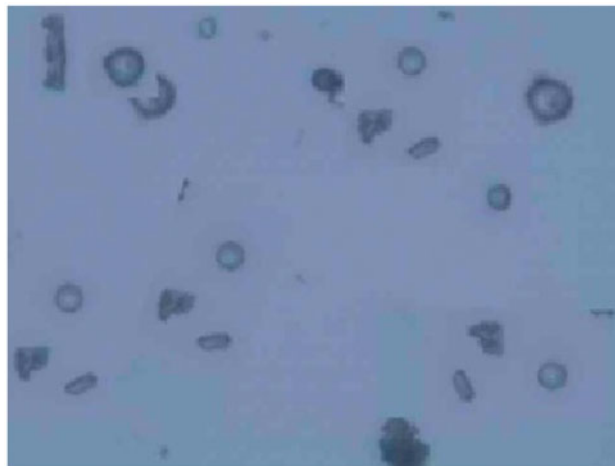


Figure 7. Photomicrograph of CFG 3 powder ( $\times 400$ ).

#### Determination of density properties

The particle density was determined using a solvent pycnometric method with acetone as the displacement fluid. The bulk density of each powder was determined by pouring 30 g of the sample at an angle of  $45^\circ$  into a 100 mL measuring cylinder with a known internal diameter. The quotient of the weight and volume was taken as bulk density. The powder in the measuring cylinder was tapped 100 times at a tap height of 2.5 cm to allow for total removal of air, onto a wooden base padded with folded cloth. The weight volume quotient was taken as the tapped density. The result recorded was the average of three determinations.

#### Determination of flow properties

The flow properties of the excipients were assessed by the angle of repose and Hausner's ratio (HR). The angle of repose which is the maximum angle that can be obtained between the self-supporting cone of the powder mound and the horizontal plain was determined according to the relationship:

$$\theta = \tan^{-1} \left( \frac{h}{r} \right) \quad (6)$$

where

$h$  = height of powder pile or cone (cm)

$r$  = radius of the cone base (cm)

$\theta$  angle of repose

The  $HR^{20}$  was determined from the bulk and tapped volumes according to the relationships:

$$HR = \frac{V_b}{V_t} \quad (7)$$

where

$V_t$  = tapped volume ( $\text{cm}^3$ )

$V_b$  = bulk volume ( $\text{cm}^3$ )

#### Determination of packing and cohesive properties

The packing and cohesive properties of the excipients were determined by pouring 30 g of the samples into a 100 mL measuring cylinder with a known internal diameter at angle  $45^\circ$ . The cylinder was tapped 100 times at a standard rate of 38 taps per minute<sup>21</sup> and the volume of the powder bed was recorded at 20, 40, 60, 80 and 100 taps each. The packing properties were obtained using a modification of Kawakita equation<sup>6,22</sup>

$$\frac{N}{C} \frac{1}{a} \frac{1}{b} \quad (8)$$

where  $a$  and  $b$  are constants,  $N$  is the number of taps and  $C$  denotes the degree of volume reduction due to tapping and can be calculated from Equation (10).

$$C = \frac{V_o - V_N}{V_o} \quad (9)$$

where  $V_o$  and  $V_N$  are the powder bed volumes at initial and  $n$ th tapped states, respectively.

### Determination of consolidation index and rate of consolidation

These were determined by using the method described by Neumann et al.<sup>23</sup> to study the relative decrease in powder volume and density change as a function of applied load.

$$\log(\rho_{td} - \rho_{bd}) = K \log N + C \quad (10)$$

where  $K$  and  $C$  are constants denoting the rate of consolidation and consolidation index (CI), respectively,  $N$  is the number of taps, while  $\rho_{bd}$  and  $\rho_{td}$  are initial bulk density and the density of the powder bed after  $N$ th tap, respectively.

### Determination of the AIF

The AIF was determined from the relationship between the porosity and the number of taps,  $N$  used to induce consolidation of the powder bed by plotting the  $\varepsilon^2 N / (1 - \varepsilon)$  (porosity factor) against  $N$ . The AIF is derived by determining the angle made between the straight line and the abscissa when  $K - K_o$  is re-plotted against  $N$ <sup>24</sup>.

$$\text{where } K = \varepsilon^2 N / (1 - \varepsilon) \quad (11)$$

$K_o$  = intercept of the plot of  $K$  against  $N$ .

$N$  = number of taps

$\varepsilon$  = porosity

### Preparation of tablets

The compressional and compaction properties of the excipients were studied by making them into compacts. The compacts were prepared by compressing 250 mg of each excipient, manually filled into the die cavity of 8 mm flat punches, at nine different pressures (156–468 MNm<sup>-2</sup>). Six compacts were prepared at each compression force and stored over silica gel for 48 h to allow elastic recovery and hardening, and to prevent falsely low yield values. The compacts were evaluated for thickness, diameter and weight uniformity.

### Heckel analysis

The compression behaviour of the excipients was characterized using the Heckel model<sup>25,26</sup>, as shown in Equation (12);

$$\ln \frac{1}{1 - D} = kP + A \quad (12)$$

where  $D$  is the relative density of the tablets at applied pressure  $P$  and  $K$  is the material dependent constant, i.e. the slope of the straight line portion of the Heckel plot and the reciprocal of  $K$  is the mean yield pressure ( $P_y$ ).

### Porosity

Porosity was calculated based on the apparent density and the true density of the compacted powders. Porosity ( $\varepsilon$ ) was calculated based on the mathematical equation:

$$\varepsilon = 1 - \frac{\text{Apparent density}}{\text{True density}} \quad (13)$$

### Hardness and tensile strength

The tensile strength of the compacts was determined using the method of Fell and Newton<sup>27</sup>. An Erweka digital hardness tester (G.B CALEVA, Dorset, England) was used at room temperature to determine the force required to diametrically break the tablets (crushing strength) into two equal halves. The tensile strength ( $T$ ) was then calculated according to formula:

$$T = \frac{2F}{\pi dt} \quad (14)$$

where  $F$  denotes the crushing strength (N),  $d$  and  $t$  are the tablet diameter (m) and thickness (m), respectively.

### Dilution potential

Compacts weighing 250 mg and containing binary mixtures of each of the excipients with paracetamol were prepared such that each of the 250 mg tablets contained paracetamol and the excipients in ratios (80:20; 60:40; 40:60; 20:80; 0:100). The compacts were prepared by compressing the binary mixtures at a compression pressure of 429 MNm<sup>-2</sup> on a Carver hydraulic hand press (Carver, IN) using a 8 mm flat-faced punches and die, lubricated with a 2% w/v dispersion of magnesium stearate and talc (1:1) in acetone before each compression. After ejection, the tablets were stored over silica gel for 48 h to allow for elastic recovery and hardening, and to prevent falsely low yield values during analysis. The force required to diametrically break the tablets (crushing strength) into two equal halves was determined using the Erweka digital hardness tester at room temperature and the tensile strength (MNm<sup>-2</sup>) was then calculated according to Equation (14).

### Results and discussion

The geometric and morphological properties of the excipients are presented in Table 1. The method employed in particle engineering has been reported to affect the morphologic properties of the resulting excipients<sup>28–30</sup>. AR varies between 0 and 1, with a perfect circle having an AR of 1, while particles with elongated shape have their AR values closer to 0. ER is the inverse of AR. RD is a measure of how the projected area of the particle resembles that of a perfect circle with a perfect circle having a RD of 1. IR measures the surface area compared to the size of the particle with a perfect circle having an IR of  $\pi$ <sup>19,31</sup>.

AR and ER values show a rank order for sphericity of TPS > GTM > CFG 1 > CFG 2 > MNT > CFG 3 > FTM. TPS granules have been reported in literature to have spherical shape<sup>17</sup>. The photomicrographs presented in Figures 1–7 showed that MNT and FTM have elongated needle-like shapes while TPS, GTM, CFG 1, CFG 2 and CFG 3 produced varying degrees of sphericity, ranging from oval to round. The high

Table 1. The geometric and morphological properties of native and coprocessed excipients.

Excipient	Aspect ratio (AR)	Elongation ratio (ER)	Roundness (RD)	Irregularity (IR)	Equivalent circle diameter (ECD) ( $\mu$ m)
MNT	0.69	0.31	0.81	2.75	16.52
TPS	0.83	0.17	0.83	3.05	14.88
FTM	0.62	0.38	0.70	2.73	14.69
GTM	0.82	0.18	0.73	3.20	16.19
CFG 1	0.79	0.21	0.82	2.93	17.27
CFG 2	0.75	0.25	0.78	2.93	16.30
CFG 3	0.67	0.33	0.67	3.07	13.59

percentage of FTM in CFG 3 could have been responsible for its low AR. The method of coprocessing was found to affect the shape of the novel excipients as GTM produced particles that were spherical while FTM produced elongated needle-like particles. Further coprocessing of GTM and FTM led to a reduction in the sphericity of the particles with increase in the concentration of FTM in the novel excipients. This is shown in the AR, ER, RD values and IR. The slight differences observed in the rank order of AR, ER, RD and IR could be due to variations in parameters used to calculate them. The ECD presented in Table 1 gives an indication of the particle size of the novel excipients with a rank order of CFG 1 > MNT > CFG 2 > GTM > TPS > FTM > CFG 3; and an approximate median particle size of 13.59–17.25  $\mu\text{m}$ . The results suggest that the methods used in coprocessing the native excipients may not lead to a major difference in the particle size of the novel excipients produced.

The density and flow properties of the primary and novel excipients are presented in Table 2. The HR, angle of repose and AIF were used to assess the flow properties of the excipients. The angle of repose ( $\theta$ ) gives an indication of the inter-particle frictional forces operating within the powder system by quantifying the resistance of the powder mass to flow<sup>32</sup>. Values of  $\theta$  less than about 25° is indicative of fair to good powder flow, while values greater than about 50° suggests that the material has extremely poor flow. Generally, values below about 30° range are considered to be appropriate for solid dosage from technology<sup>33</sup>. It was observed (Table 2) that the novel excipients generally have better flow properties than the native excipients. A HR of less than 1.2 is indicative of good flowability while values of 1.5 or higher suggest poor powder flowability<sup>20</sup>. Table 2 shows that MNT and GTM have poor flow properties while TPS, FTM, CFG 1, CFG 2 and CFG 3 all have fair flow properties.

It is widely known that a complex interplay between particle size, particle shape, particle size distribution and the intra- and inter-particle forces at work within the particles makes it difficult to describe how these parameters individually affect the flowability of powders. These descriptors of powder flowability use different principles to assess this property in a powder system and do not necessarily have to correlate<sup>8,32,34</sup>. While some tests would simply yield a ranking order for powders, others are able to describe the behaviour of the powder under certain conditions thus enabling the ability to predict the behaviour of such powder during manufacturing<sup>11</sup>. A form of correlation is provided by the fact that the novel excipient, GTM, with a high value of HR, also had the highest angle of repose among the coprocessed excipients. This suggests that co-grinding was less effective than co-fusion in the production of novel excipients with enhanced flowability.

Plots of N/C against the number of taps as shown in Figure 8 gave a linear relationship with correlation  $r > 0.972$ . Values of  $a$ , i.e. the maximum volume reduction after tapping, obtained from the slope of the straight lines are presented as percentages in Table 3. The rank order of “ $a$ ” is MNT > GTM > TPS > CFG

2 > CFG 1 > CFG 3 > FTM. A low value of  $a$  indicates that the powder system has packed more densely on initial pouring into the cylinder, which implies that the powders were well packed before tapping, since tapping did not give considerable improvement in their packing. For powders with low “ $a$ ”, tapping reduces the voids by displacing air from the powder bed, without changing the size and shape of the particles<sup>6</sup>. Ilic et al.<sup>34</sup> in their study on powder particle rearrangement suggested that powders with “ $a$ ” less than 21% have good flowability while those greater than 41% have poor flowability. The result presented in Table 3 showed that

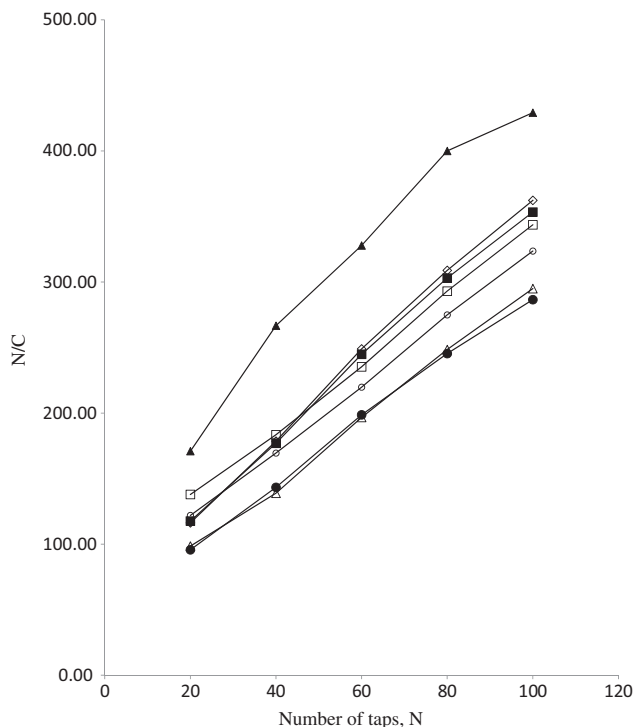


Figure 8. Modified Kawakita plot for disintegrant samples; MNT (●), TPS (○), FTM (▲), GTM (Δ), CFG 1 (■), CFG 2 (□), CFG 3 (◇).

Table 3. Packing, consolidation and compaction properties and mean yield pressure of the native and coprocessed excipients.

Excipients	Maximum volume reduction ( $a$ )	Consolidation index (CI)	Rate of consolidation (K)	Mean yield pressure ( $P_y$ )
MNT	41.3	-1.071	0.3093	158.73
TPS	39.3	-1.277	0.3919	140.85
FTM	30.8	-1.484	0.4186	181.82
GTM	39.8	-1.065	0.3049	163.93
CFG 1	33.5	-1.156	0.3063	169.49
CFG 2	38.4	-1.373	0.4279	172.41
CFG 3	32.1	-1.119	0.2821	178.57

Table 2. Density and flow properties of native and coprocessed excipients.

Excipient	Bulk density ( $\text{g}/\text{cm}^3$ )	Tapped density ( $\text{g}/\text{cm}^3$ )	Particle density ( $\text{g}/\text{cm}^3$ )	Angle of repose	Hausner's ratio	Angle of internal friction
MNT	0.349 (0.007)*	0.534 (0.021)	1.517 (0.011)	30.68	1.530	46.65
TPS	0.546 (0.008)	0.791 (0.038)	1.455 (0.004)	30.82	1.449	17.42
FTM	0.500 (0.012)	0.661 (0.035)	1.389 (0.018)	20.03	1.321	28.38
GTM	0.512 (0.030)	0.780 (0.026)	1.431 (0.018)	21.46	1.525	18.44
CFG 1	0.564 (0.018)	0.795 (0.020)	1.377 (0.004)	18.08	1.411	15.22
CFG 2	0.551 (0.006)	0.775 (0.026)	1.327 (0.027)	19.28	1.307	13.49
CFG 3	0.522 (0.012)	0.724 (0.022)	1.302 (0.015)	17.91	1.386	18.12

\*\*Figures in parenthesis are standard deviations of the mean.

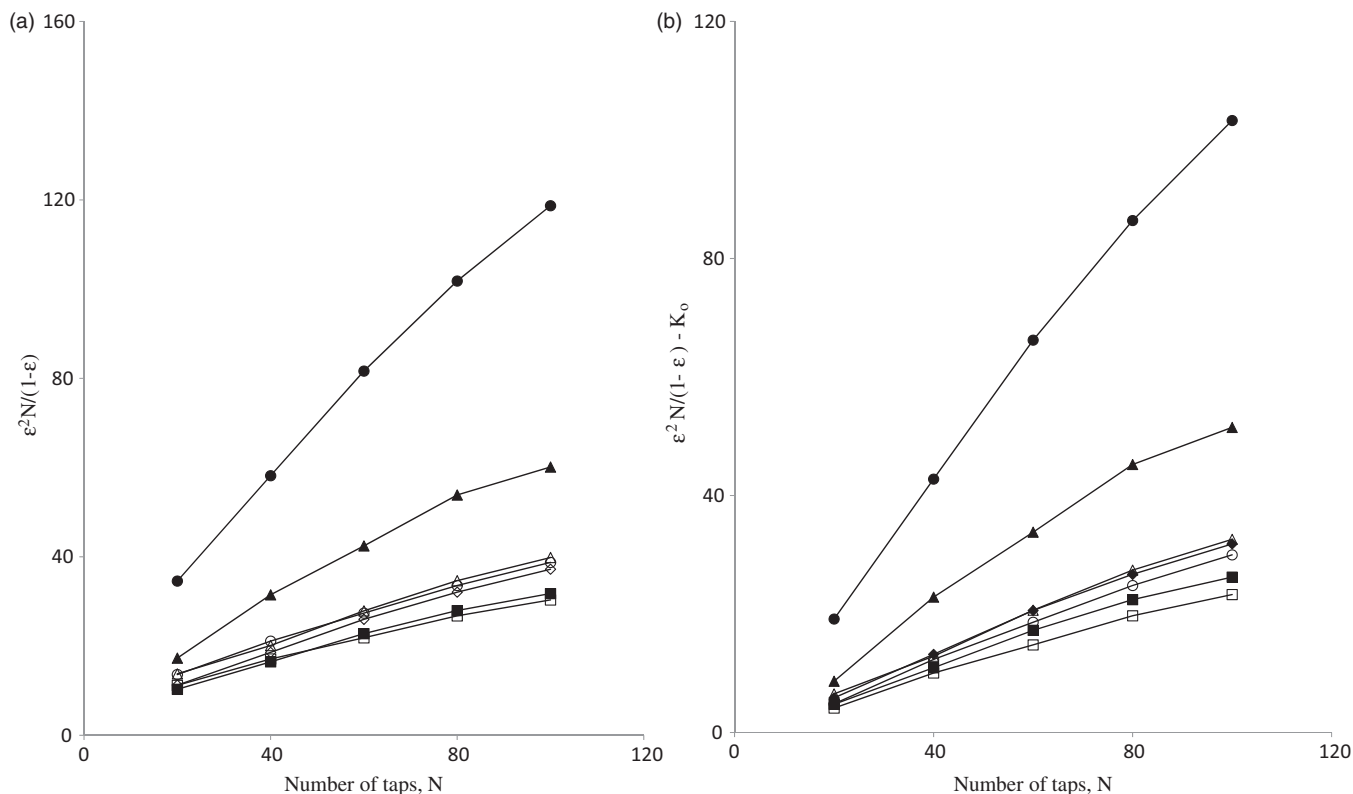


Figure 9. (a) Plots of  $\varepsilon^2 N / (1 - \varepsilon)$  against number of taps, N; MNT (●), TPS (○), FTM (▲), GTM (△), CFG 1 (■), CFG 2 (□), CFG 3 (◇). (b) Plots of  $[\varepsilon^2 N / (1 - \varepsilon)] - K_0$  against number of taps, N; MNT (●), TPS (○), FTM (▲), GTM (△), CFG 1 (■), CFG 2 (□), CFG 3 (◇).

apart from GTM, the novel excipients have improved flowability compared to native excipients.

Ludde and Kawakita<sup>35</sup> reported that the value of  $a$  was smallest for spherical particles and largest for irregular particles. Podczek and Sharma<sup>13</sup> also observed that a reduction in particle size resulted in an increase in the value of  $a$ . However, it is important to note that no general rule exists to explain the influence of these two parameters on packing and cohesive properties since they can interact at varying degrees to modulate the behaviour of powder systems. Thus, it can be observed from Tables 1 and 3 that MNT with the highest particle size, exhibited the highest value of  $a$ , suggesting that the elongated shape of MNT played a major role than its particle size in its observed packing behaviour, since the area of contact within the powder bed would be higher in elongated particles compared to spherical particles. However, FTM and CFG 3 having the most elongated shapes with AR values of 0.62 and 0.67, respectively, exhibited the lowest amount of packing due to tapping suggesting that particle shape did not influence the packing behaviour of the excipients. It is possible that the use of heat in its preparation resulted in strong particles<sup>36</sup> with high shear strength that were resistant to change shape due to shearing during tapping, resulting in the formation of less dense plugs. Relative changes in the packing behaviour have been thought to be sensitive indicators of the structural strength of a loosely compacted powder and its subsequent flow characteristics in many process operations<sup>37</sup>. For TPS and GTM, the most spherical of the excipients, it was observed that TPS with a smaller particle size exhibited a lower amount of volume reduction than GTM suggesting that particle shape influenced the packing behaviour since TPS was more spherical than GTM. On further coprocessing of GTM and FTM, it was observed that an increase in the concentration of FTM in the novel excipients reduced the values of  $a$ , angle of repose and particle size, thus suggesting that it was the nature of the FTM and not

particle size and shape, that affected packing behaviour of the excipients.

Powder flow involves frictional contact of individual particles. The area of contact, the magnitude and strength of attractive forces between contacting particles and the amount of shearing and rupture at the contact points of particles all contribute to influence the flowability of the powder system<sup>12</sup>. This inter-particle friction has been demonstrated to significantly affect powder packing<sup>38</sup> and the AIF is important when considering the flow of powders from the hopper into the die during tableting<sup>24</sup>. Table 2 shows the AIF for all the excipients. The AIF was obtained from Figures 9(a and b), based on Equation (12). It was observed that the novel excipients have a reduced AIF leading to improved flow of the excipients. It was also observed that TPS had a low AIF which could have been due to the slippery nature of the excipient and its potential as a lubricant<sup>17</sup>. This further illustrates the different principles guiding these methods of assessing powder flowability. The rank order for AIF is MNT > FTM > GTM > CFG 3 > TPS > CFG 1 > CFG 2. A higher value of the AIF denotes greater cohesiveness and a higher potential for the formation of bridges and arches in the powder which would impair flow<sup>19,25,39</sup>.

Figure 10 shows the relationship between the log of density changes and log number of taps. This relationship elucidates the consolidation behaviour (CI and rate of consolidation) of powder systems which provides an insight into the inter-particle movements during vibration or tapping. While a high value of CI is indicative of a cohesive powder system, low values are indicative of fluidity within the powder bed and give an indication of the ability of the particles in the powder bed to undergo rearrangement more easily during tapping or vibration and thus more easily achieve optimum packing of the powder bed. As shown in Table 3, the rank order for CI is GTM > MNT > CFG 3 > CFG 1 > TPS > CFG 2 > FTM. It was observed that GTM and MNT

exhibited the highest values of CI, while FTM exhibited the lowest, thus suggesting a higher cohesive property of GTM and MNT particles and the propensity of FTM particles to reshuffle and fill void spaces during tapping. The low value of CI for FTM could have been responsible for its low  $a$  values. The rate of consolidation provides a measure of the rate of packing of the particles when subjected to tapping or vibration. The rank order of the rate of consolidation is CFG 2 > FTM > TPS > MNT > CFG 1 > GTM > CFG 3.

The compaction data were analysed using the Heckel model. Tableability, compressibility and compactability are shown in Figures 11–15. Heckel analysis is a method for transforming a parametric view of the force and displacement signals to a linear relationship for materials undergoing compaction. The equation is based on the assumption that the dependence of densification on compaction pressure is first order<sup>3,39</sup>. Values of mean yield pressure  $P_y$  (Table 3) were calculated from the region of the plots (Figure 14) showing the highest correlation coefficient for linearity of >0.93 for all excipients. A rank order of FTM > CFG 3 > CFG 2 > CFG 1 > GTM > MNT > TPS was observed for the  $P_y$ . This implies that the onset of plastic deformation is faster in the native than the coprocessed excipients. High  $P_y$  is indicative of higher yield strength, requiring higher forces of compaction to initiate deformation. This may not be desirable for high speed tableting machines where minimum dwell time is available for compression of powders to form compacts.

The ability of a powder to form a compact with sufficient mechanical properties under the effect of compression pressure is known as tableability<sup>40</sup>. The plots of tensile strength against applied compaction pressure as shown in Figure 11 describe the tableability of the native and novel excipients. Generally, the tableability of all the test excipients improved with an increase in compaction pressure. This could be due to the reduction of the tablet porosity and the increase in particle–particle contact points available for bond formation. The tensile strength of the

coprocessed excipients was compared with that of the native excipients. The excipients TPS and MNT showed tensile strength values of 0.27 and 1.06, respectively, in comparison with FTM (4.09), GTM (0.64), CFG 1 (1.52), CFG 2 (1.78) and CFG 3

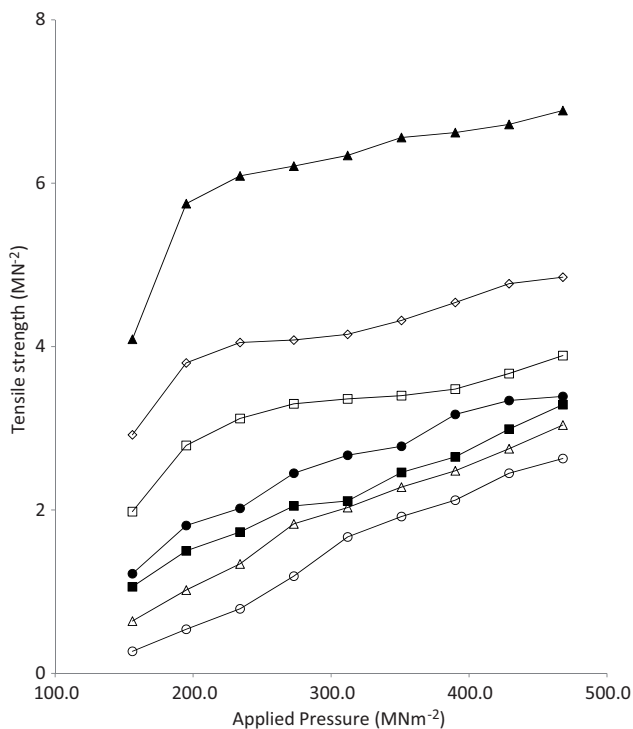


Figure 11. Plots of tensile strength ( $T$ ) against applied pressure ( $\text{MNm}^{-2}$ ), MNT (●), TPS (○), FTM (▲), GTM (△), CFG 1 (■), CFG 2 (□), CFG 3 (◇).

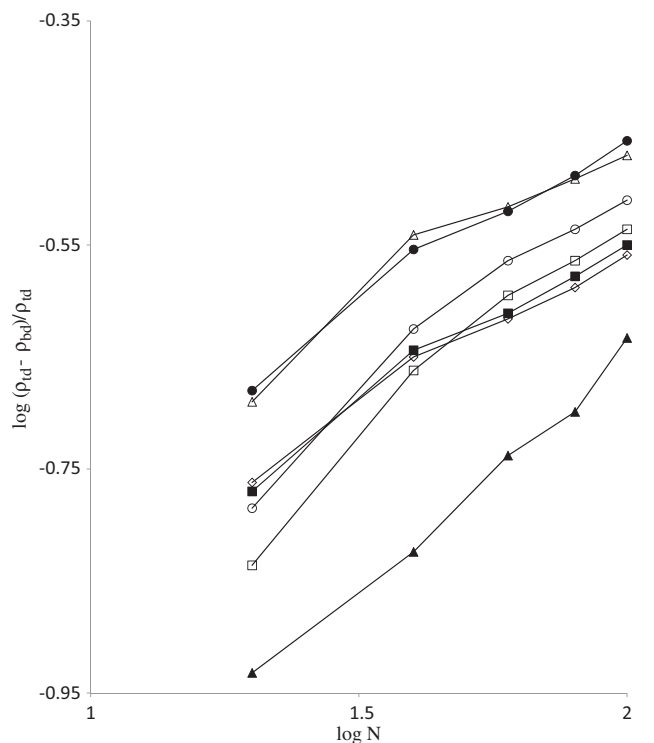


Figure 10. Plots of  $\log(\rho_{td} - \rho_{bd})/\rho_{td}$  against  $\log$  number of taps,  $N$ ; MNT (●), TPS (○), FTM (▲), GTM (△), CFG 1 (■), CFG 2 (□), CFG 3 (◇).

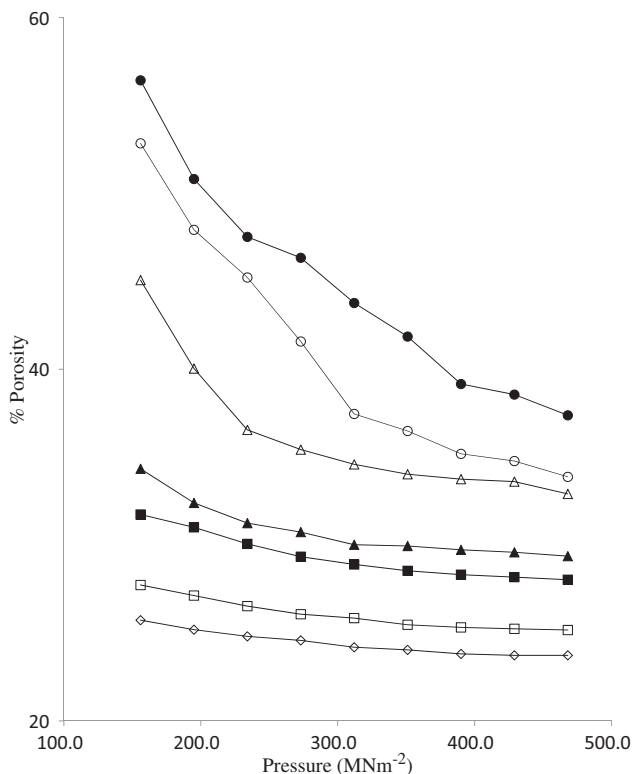


Figure 12. Plots of percentage porosity against applied pressure ( $\text{MNm}^{-2}$ ), MNT (●), TPS (○), FTM (▲), GTM (△), CFG 1 (■), CFG 2 (□), CFG 3 (◇).



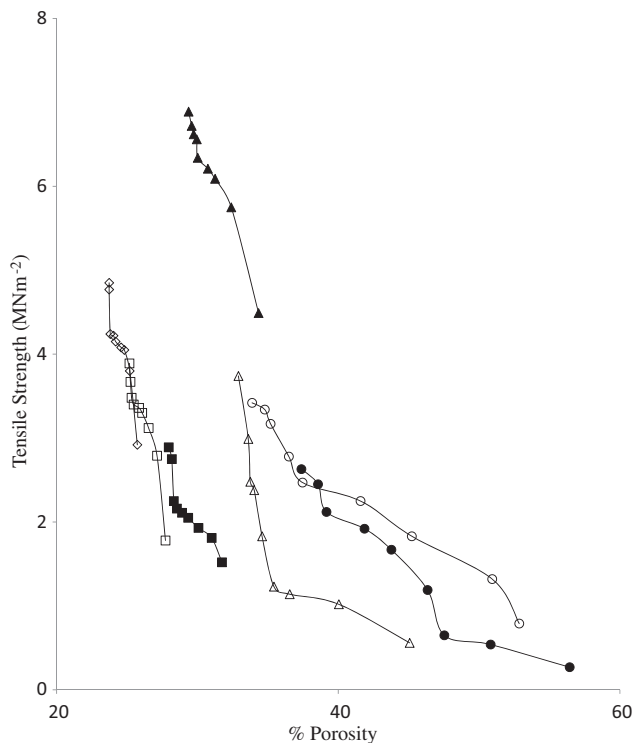


Figure 13. Plots of tensile strength ( $T$ ) against percentage porosity, MNT (●), TPS (○), FTM (▲), GTM (△), CFG 1 (■), CFG 2 (□), CGF 3 (◇).

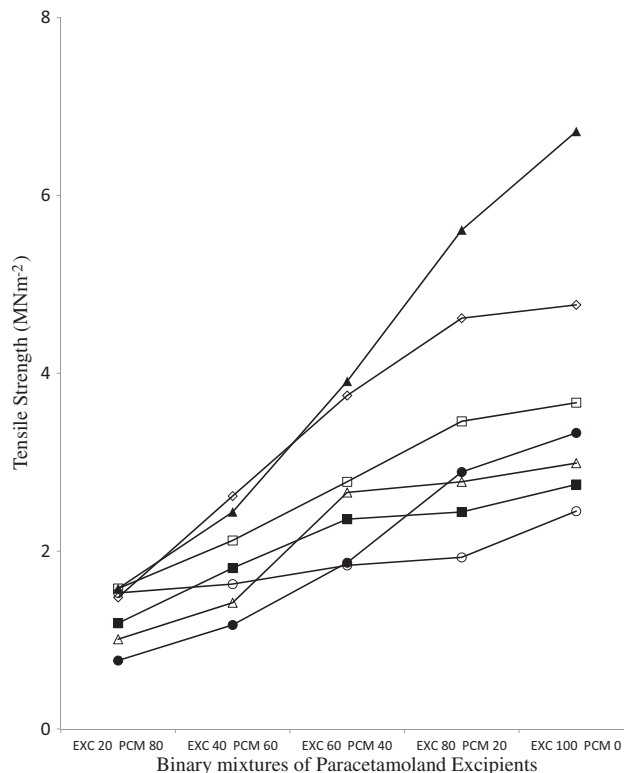


Figure 15. Plots of tensile strength ( $T$ ) against applied pressure ( $\text{MNm}^{-2}$ ) for binary mixtures of paracetamol and excipients, MNT (●), TPS (○), FTM (▲), GTM (△), CFG 1 (■), CFG 2 (□), CGF 3 (◇).

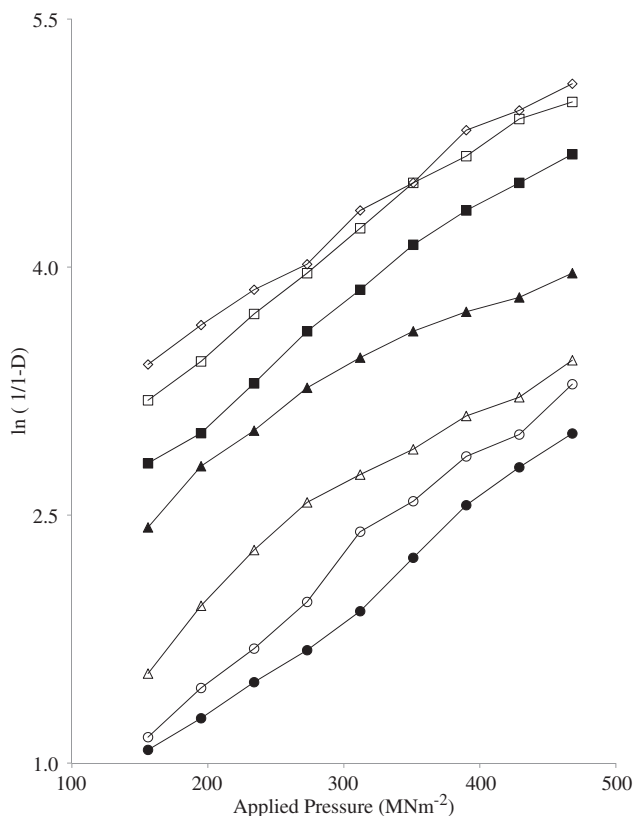


Figure 14. Plots of  $\ln(1/(1-D))$  against applied pressure ( $\text{MNm}^{-2}$ ), MNT (●), TPS (○), FTM (▲), GTM (△), CFG 1 (■), CFG 2 (□), CGF 3 (◇).

(2.92) at  $156.0 \text{ MNm}^{-2}$  compaction pressures. However, a slightly different trend was observed at  $273.0\text{--}468.0 \text{ MNm}^{-2}$  compaction pressures, where the tensile strength decreased in the order  $\text{FTM} > \text{CFG 3} > \text{CFG 2} > \text{MNT} > \text{CFG 1} > \text{GTM} > \text{TPS}$

(Figure 11). The needle-like shape of MNT and its ability to undergo fragmentation which would lead to mechanical interlocking could have contributed to its high tabletability while the low tabletability of TPS can be attributed to its spherical shape. The AR values presented in Table 1 showed a decrease in tabletability with increase in AR values. This could be due to the ability of particles with elongated shape to undergo an initial absorbance of other particles and a consequent particle–particle interlocking. It was also observed that excipients with elongated particles allowed for a higher gradient of the first two points of the plot on Figure 11, before an upward trend towards a plateau. For more spherical excipients like TPS, GTM and CFG 1, this high gradient between the first two points was absent.

Powder compressibility refers to the ability of a material to reduce in volume<sup>39</sup>. The plot of porosity against applied compaction pressure is shown in Figure 12. The values of porosity obtained at the lowest compression pressure ( $156 \text{ MNm}^{-2}$ ) were TPS (52.85%), MNT (56.43%), FTM (34.34%), GTM (45.07%), CFG 1 (31.78%), CFG 2 (27.78%) and CFG 3 (25.73%); while the values of porosity obtained at the highest compression pressure ( $468.0 \text{ MNm}^{-2}$ ) were TPS (37.38%), MNT (33.88%), FTM (29.37%), GTM (32.91%), CFG 1 (28.03%), CFG 2 (25.17%) and CFG 3 (23.73%). A higher reduction in porosity observed in TPS, MNT and GTM suggests a higher initial powder volume and an initial particle rearrangement phase when the compaction pressure is applied. This supports the result obtained from the “ $a$ ” values of the modified Kawakita plots where TPS, MNT and GTM underwent higher volume reduction. A highly compressible powder enables particles to get closer to each other, thus facilitating interparticulate bonding and the formation of stronger compacts. It was also observed that the compressibility of FTM, CFG 3, CFG 2 and CFG 1 was less dependent on applied compaction pressure (Figure 12), as the change in compaction pressure from 156 to  $468 \text{ MNm}^{-2}$  was small. This suggests a

lower initial powder volume and enhanced particle arrangement that eliminated air vacuoles and facilitated closer particle contact and the formation of stronger bonds.

Compactability, which is the ability to produce tablets with sufficient tensile strength under the effect of densification<sup>40</sup> can be studied using tensile strength–porosity profiles as shown in Figure 13. The tensile strength of the compacts increased as the porosity of the compacts reduced. It was however observed that the change in tensile strength for FTM, CFG 1, CFG 2 and CFG 3 was not completely dependent on a reduction of porosity within the compact. This suggests that the ability of these excipients to form stronger bonds was more influential than compact porosity in their observed compact tensile strength. Particle shape dependent compactability behaviour was also observed for all the test excipients except MNT. The tensile strength of the compacts increased with a decrease in AR values. The low bulk density of MNT could have been responsible for its observed higher porosity.

Dilution potential, an important property of excipient for direct compression, is used to measure the amount of drug substance that can be incorporated into a tablet while still maintaining satisfactory mechanical properties with respect to hardness and/or friability. Generally, the more the drug that can be added to an excipient, the higher the dilution potential<sup>1</sup>. The choice of paracetamol was based on its poor compaction property and its ability to undergo considerable elastic recovery after withdrawal of the compression pressure<sup>41</sup>. Generally, the mechanical strength of the compacts increased as the ratio of the excipients relative to the drug increased. It is seen in Figure 15 that both the native and coprocessed excipients were shown to have high dilution potential with tensile strengths values greater than 0.77 and 1.17 MNm<sup>-2</sup> at 20:80 and 40:60 excipients–paracetamol mixtures, respectively. The dilution potential of the test excipients corresponds to the observed tabletability and compactability behaviour of the excipients. The effects of particle shape and bond formation on these properties could have played an important role in the observed dilution potential behaviour of the excipients.

## Conclusion

The results obtained from this work showed that:

- TPS and MNT can be coprocessed to produce novel excipients with enhanced flow, packing and compaction properties;
- the method of coprocessing employed, i.e. co-fusion or co-grinding would affect the morphological, physical and compaction properties of the novel excipients;
- the morphological and physical properties influenced the flow, packing and compaction properties of the novel excipients;
- the resulting products' potential as direct compressible excipients was greater than those of the starting materials; this is reflected in the tabletability, compressibility, compactability and dilution potential results obtained;
- pharmaceutical powder of a multidimensional nature will require the use of various bulk powder descriptors to elucidate the mechanism of their flow and packing behaviour and;
- co-fusion as a coprocessing method would produce novel excipients with enhanced direct compression potential compared to the co-grinding method.

## Declaration of interest

The authors report no declarations of interest.

## References

1. Gohel MC, Jogani PD. A review of co-processed directly compressible excipients. *J Pharm Pharmaceut Sci* 2005;8:76–93.

2. Saha S, Shahiwala AF. Multifunctional coprocessed excipients for improved tableting performance. *Exp Opin Drug Deliv* 2009;6:197–208.
3. Barot BS, Parejiya PB, Patel TM, et al. Compactability improvement of metformin hydrochloride by crystallization technique. *Adv Powder Technol* 2012;23:814–823.
4. Gonnissen Y, Remon JP, Vervaet C. Development of directly compressible powders via co-spray drying. *Eur J Pharm Biopharm* 2007;67:220–226.
5. Adeagbo AA, Alebiowu G. Evaluation of cocoa butter as potential lubricant for co-processing in pharmaceutical tablets. *Pharm Dev Technol* 2008;13:197–204.
6. Maghsoodi M, Hassan-Zadeh D, Barzegar-Jalali M, et al. Improved compaction and packing properties of naproxen agglomerated crystals obtained by spherical crystallization technique. *Drug Dev Ind Pharm* 2007;33:1216–1224.
7. Schneider LCR, Sinka IC, Cocks ACF. Characterisation of the flow behaviour of pharmaceutical powders using a model die–shoe filling system. *Powder Technol* 2007;173:59–71.
8. Vasilenko A, Glasser BJ, Muzzio FJ. Shear and flow behaviour of pharmaceutical blends – method comparison study. *Powder Technol* 2011;208:628–636.
9. Shinohara K, Oida M, Golman B. Effect of particle shape on angle of internal friction by triaxial compression test. *Powder Technol* 2000;107:131–136.
10. Suzuki M, Sato H, Hasegawa M, Hirota M. Effect of size distribution on tapping properties of fine powder. *Powder Technol* 2001;118:53–57.
11. Sandler N, Wilson D. Prediction of granule packing and flow behaviour based on particle size and shape analysis. *J Pharm Sci* 2010;99:958–968.
12. Podczeczek F, Miah Y. The influence of particle size and shape on the angle of internal friction and the flow factor of unlubricated and lubricated powders. *Int J Pharm* 1996;14:187–194.
13. Podczeczek F, Sharma M. The influence of particle size and shape of components of binary powder mixtures on the maximum volume reduction due to packing. *Int J Pharm* 1996;137:41–48.
14. Alebiowu G, Adeyemi AO. Influence of starch steeping period on the dimensionless disintegration values of a paracetamol tablet formulation. *Acta Pol Pharm Drug Res* 2009;66:311–320.
15. Alebiowu G, Osinoiki KA. Assessment of tapioca starches obtained after different steeping periods as binders in a paracetamol tablet formulation. *Farmacia* 2010;58:341–352.
16. Nassab PR, Rajko R, Szabo-Revesz P. Physicochemical characterization of meloxicam–mannitol binary systems. *J Pharm Biomed Anal* 2006;41:1191–1197.
17. Alebiowu G. Steeping period influence on physical, compressional and mechanical properties of tapioca starch. *J Pharm Res* 2007;6:139–144.
18. Sharma V, Philip AK, Pathak K. Modified polysaccharides as fast disintegrating excipients for orodispersible tablets of roxithromycin. *AAPS Pharm Sci Technol* 2008;9:87–94.
19. Ogunjimi AT, Alebiowu G. Flow and consolidation properties of neum gum coprocessed with two pharmaceutical excipients. *Powder Technol* 2013;246:187–192.
20. Hausner HH. Friction conditions in a mass of metal powder. *Int J Powder Metall* 1967;3:7–13.
21. British Standards Institution. BS 1460:1967: Method for determination of apparent density after compaction of precipitated calcium carbonate; 1967.
22. Kawakita K, Tsutsumi YA. Comparison of equations for powder compression. *Bull Chem Soc Jpn* 1966;39:1364–1368.
23. Neumann BS, Bean HS, Becket AH, Carless JE. *Advances in pharmaceutical sciences*. Vol. 2. London: Academic Press; 1967.
24. Varthalis S, Pilpel N. Anomalies in some properties of powder mixtures. *J Pharm Pharmacol* 1976;28:415–419.
25. Heckel RW. Density–pressure relationships in powder compaction. *Trans Metall Soc AIME* 1961;221:671–675.
26. Heckel RW. An analysis of powder compaction phenomena. *Trans Metall Soc AIME* 1961;221:1001–1008.
27. Fell JT, Newton JM. Determination of tablet strength by diametral compression test. *J Pharm Sci* 1970;59:688–691.
28. Rahmati MR, Vatanara A, Parsian AR, et al. Effect of formulation ingredients on the physical characteristics of salmeterol xinafoate microparticles tailored by spray freeze drying. *Adv Powder Technol* 2013;24:36–42.

29. Tewa-Tagne T, Braincon S, Fessi H. Preparation of redispersible dry nanocapsules by means of spray drying: development and characterization. *Eur J Pharm Sci* 2007;30:124–135.
30. Kawase M, Muira K. Fine particle synthesis by continuous precipitation using a tubular reactor. *Adv Powder Technol* 2007; 18:725–738.
31. Amidon GE, Secreast PJ, Mudie D. Particle, powder, and compact characterization. In: Qiu Y, Chen Y, Zhang GGZ, et al, eds. *Developing solid oral dosage forms; pharmaceutical theory and practice*. New York: Elsevier Inc; 2009:163–186.
32. Staniforth JN, Aulton ME. Powder flow. In: Aulton ME, ed. *Pharmaceutics: the design and manufacture of medicines*. 3rd ed. New York: Elsevier; 2007:168–178.
33. Zhou Q, Armstrong B, Larson I, et al. Improving powder flow properties of a cohesive lactose monohydrate powder by intensive mechanical dry coating. *J Pharm Sci* 2010;99:969–981.
34. Ilic I, Kása Jr P, Dreu R, et al. The compressibility and compactibility of different types of lactose. *Drug Dev Ind Pharm* 2009;35:1271–1280.
35. Ludde KH, Kawakita K. Die Pulver compression. *Pharmazie* 1966; 21:393–403.
36. Alebiowu G, Itiola OA. Compressional characteristics of native and pregelatinized forms of sorghum, plantain, and corn starches and the mechanical properties of their tablets. *Drug Dev Ind Pharm* 2002;28: 663–672.
37. Abdullah EC, Geldart D. The use of bulk density measurements as flowability indicators. *Powder Technol* 1999;102:151–165.
38. Zhang ZP, Liu LF, Yuan YD, Yu AB. A simulation study of the effects of dynamic variables on the packing of spheres. *Powder Technol* 2001;116:23–32.
39. Okore VC. A preliminary study of Dika fat treated talc as a glidants for model granulations. *W Afric J Pharm* 1999;12:30–33.
40. Joshi AB, Patel S, Kaushal AM, Bansal AK. Compaction studies of alternate solid forms of celecoxib. *Adv Powder Technol* 2010;21: 452–460.
41. Alderborn G, Nyström C. Radial and axial tensile strength and strength variability of paracetamol tablets. *Acta Pharma Seuc* 1984; 21:1–8.